Investigation of the Electropolymerization of *o*-Toluidine and *p*-Phenylenediamine and Their Electrocopolymerization by *In Situ* Ultraviolet–Visible Spectroelectrochemistry

Guirong Zhang, Aijian Zhang, Xiuli Liu, Shufeng Zhao, Jingbo Zhang, Jiaxing Lu

Shanghai Key Laboratory of Green Chemistry and Chemical Process, Department of Chemistry, East China Normal University, Shanghai 200062, People's Republic of China

Received 2 June 2008; accepted 19 October 2008
DOI 10.1002/app.29597
Published online 26 October 2009 in Wiley InterScience (www.interscience.wiley.com).

ABSTRACT: Under the conditions of potentiostatic electrolysis, the electropolymerization of *o*-toluidine (OT) and *para*-phenylenediamine (PPDA) and the electrocopolymerization between OT and PPDA on an indium tin oxide (ITO) conductive glass electrode at potentials of 0.7, 0.8, and 0.9 V were studied in detail by *in situ* ultraviolet–visible (UV–vis) spectrometry in 0.5 mol/L sulfuric acid media. It was shown that both OT and PPDA could be electropolymerized on the ITO electrode, which depended on the applied electrolysis potential and the concentration of the monomer. Furthermore, *in situ* UV–vis spectra indicated that the electrocopolymerization between OT and PPDA could happen. The presence of PPDA not only promoted polymerization but also accelerated polymerization, which was attributed to the formation of an intermediate result from the coupling of PPDA and the toluidine monomer cation radical. PPDA could be incorporated into the copolymer to make the copolymer have a phenazine or phenazine-like cyclic structure, which was proven by the reflectance Fourier transform infrared spectra of the polymer and copolymer. The scanning electron microscopy morphology images of the polymers obtained showed that, in addition to accelerating polymerization, PPDA also could change the method of nucleation for the polymer to make the copolymer possess a fibrous surface morphology. The diameter of the fibroid copolymer was about 100 nm, and the length of that reached about 1000 nm. In the article, a newer concerned mechanism of copolymerization was proposed. © 2009 Wiley Periodicals, Inc. J Appl Polym Sci 115: 2635–2647, 2010

Key words: copolymerization; electrochemistry; FTIR; reactive processing; UV–vis spectroscopy

INTRODUCTION

For more than 20 years, polyaniline, as a very hopeful conducting polymer with many potential advanced applications,[1–7] has attracted considerable attention because of its relatively easy preparation, excellent environmental stability, and good acidic and electric dopabilities. The conductivity of polyaniline comes from its delocalized π-conjugated bond, but the structure of polyaniline also leads to its lack of solubility in organic solvents and its poor processable properties, which have restricted its practical utility. To overcome these difficulties, there are two important approaches employed to improve the properties of polyaniline conductive polymers: one is to polymerize substituted anilines, such as *N*-substituted and aromatic-ring-substituted anilines, with chemical and electrochemical methods; the other is to produce some special copolymers between different aniline derivatives through the two methods mentioned previously. In particular, not only could the copolymerization approach tune the properties of copolymers by changing the ratio of different monomer concentrations in the copolymerization system bath,[8] but also the structural information of copolymers and homopolymers might be acquired through a comparison of the characteristics, that is, through Fourier transform infrared (FTIR) spectra, Raman spectra, scanning electron microscopy (SEM) images, and ultraviolet–visible (UV–vis) spectra, of copolymers with those of the homopolymers. Furthermore, the studies on copolymerization provide more knowledge about the reactivity of monomers and the mechanism of homopolymerization/copolymerization with *in situ* FTIR spectra, *in situ* UV–vis spectra, and so on. For this reason, the copolymerization between different aniline derivatives is increasingly being paid more and more attention.

Correspondence to: J. Lu (jxlu@chem.ecnu.edu.cn).
Contract grant sponsor: Natural Science Foundation of China; contract grant number: 20573037.
Contract grant sponsor: Major Project of the Science Committee of Shanghai; contract grant number: 05JC1470.
Contract grant sponsor: Key Project for Subject Construction of Shanghai; contract grant number: B409.

© 2009 Wiley Periodicals, Inc.

Both toluidine and phenylenediamine are two of many potential derivatives of aniline; there have been a number of reports on their homopolymerization and copolymerization with other aniline derivatives with chemical and electrochemical methods.[9–17] The prepared homopolymers and copolymers from them have unique properties, including solubility, conductivity, electrochromism, and electrochemical activity, in comparison with polyaniline, which has made many researchers use them to perform tests for various applications in sensors,[18,19] corrosion inhibition,[20] and rechargeable batteries.[21] However, so far, there are few reports on the chemical or electrochemical copolymerization of *para*-phenylenediamine (PPDA) with *o*-toluidine (OT) with *in situ* UV–vis spectroelectrochemistry.

Because the intermediate formed during the polymerization of the monomers are short lived, *in situ* UV–vis spectroscopy, which, however, is interpreted somewhat ambiguously, has been known to be an effective technique for following the intermediates. There is some literature available on the detection of the intermediates formed during polymerization of aniline or aniline derivatives through UV–vis spectroscopy.[22–25] Earlier, Genies and Lapkowski[22] used UV–vis spectroscopy to follow the course of the polymerization of aniline and reported the formation of nitrenium cations as intermediates during the polymerization. Malinauskas and Holze[23–25] monitored the early stages of the electrooxidation of aniline and ring-substituted and *N*-alkyl-substituted anilines using UV–vis spectroscopy. Recently, there have also been a few reports on the processes following the early stages of electrochemical copolymerization.[26–29] In all these cases, nitrenium-type cations have been reported to be formed as intermediates, and these intermediates have reacted chemically with the neutral monomer to yield oligomers or polymers. However, until now, the mechanism of the polymerization and the copolymerization of aniline and its derivatives by chemical or electrochemical method is still debatable, which has motivated many researchers to keep doing studies in this field.

In this study, *in situ* UV–vis spectroscopy was used to follow the course of the homopolymerization of PPDA and OT and their copolymerization through electrochemical polymerization at various constant potentials (vs a saturated Ag/AgCl electrode) on optically transparent indium tin oxide (ITO) glass working electrodes. The intermediates generated during electrochemical polymerization might be monitored to obtain evidence for homopolymer/copolymer formation, which could provide some new information about the mechanism of these polymerizations. In particular, through *in situ* UV–vis spectroscopy, we propose that the formation of intermediates resulting from the coupling of PPDA and toluidine monomer cation radicals may be a main reason for the production of the copolymer and the acceleration of the copolymerization in the electrocopolymerization. Furthermore, FTIR spectra (*ex situ*) and SEM images of the homopolymers/copolymers deposited on the ITO glass electrodes suggested a molecular structure of the copolymers and proved that the copolymerization between PPDA and OT occurred. The results obtained in this study have not been previously reported in the literature.

EXPERIMENTAL

Reagent-grade OT and PPDA were used as received without any further purification. All involved solutions were prepared with double-distilled water and contained 0.5*M* H_2SO_4 (reagent grade).

The *in situ* UV–vis spectroelectrochemical studies on the homopolymerization/copolymerization of OT and PPDA were carried out with a model Cary 300 UV–vis spectrophotometer (Varian, Inc., Palo Alto, CA) controlled by a personal computer. Spectroelectrochemical experiments were done in a quartz cuvette of 1 cm path length assembled as an electrochemical cell. An optically transparent ITO-coated glass plate was the working electrode. The electrode was installed perpendicular or parallel to the light path on the basis of the different purposes of the measurements. A platinum wire was used as the counter electrode. A saturated Ag/AgCl was used as the reference electrode. Before spectroelectrochemical experiments, fresh ITO electrodes were degreased with acetone and rinsed with doubly distilled water. The concerned potentials in this article all refer to the saturated Ag/AgCl. Electrochemical polymerization was performed by constant potential electrolysis with a model 600c CHI electrochemical working station (CH Instruments, Inc., Austin, TX). The cyclic voltammograms recorded (not listed here) for the ITO electrode in 200 m*M* OT or 20 m*M* PPDA OT at scanning rate of 20 mV/s indicated that the oxidization of both OT and PPDA started at potentials of about 0.7 and 0.65 V, respectively, so three electrolysis potentials of 0.7, 0.8, and 0.9 V were chosen to carry out studies under suitable electrochemical polymerization rates. The electrocopolymerization of PPDA and OT was done for a solution containing a mixture of PPDA and OT at different concentrations. The UV–vis spectra were recorded simultaneously while constant electrolysis was performed. Then, they were analyzed through software.

After deposition, The homopolymer/copolymers deposited on the ITO glass electrodes were washed with 0.5*M* sulfuric acid and then rinsed with double-distilled water to remove any unreacted monomer. They were dried in an air atmosphere for 48 h

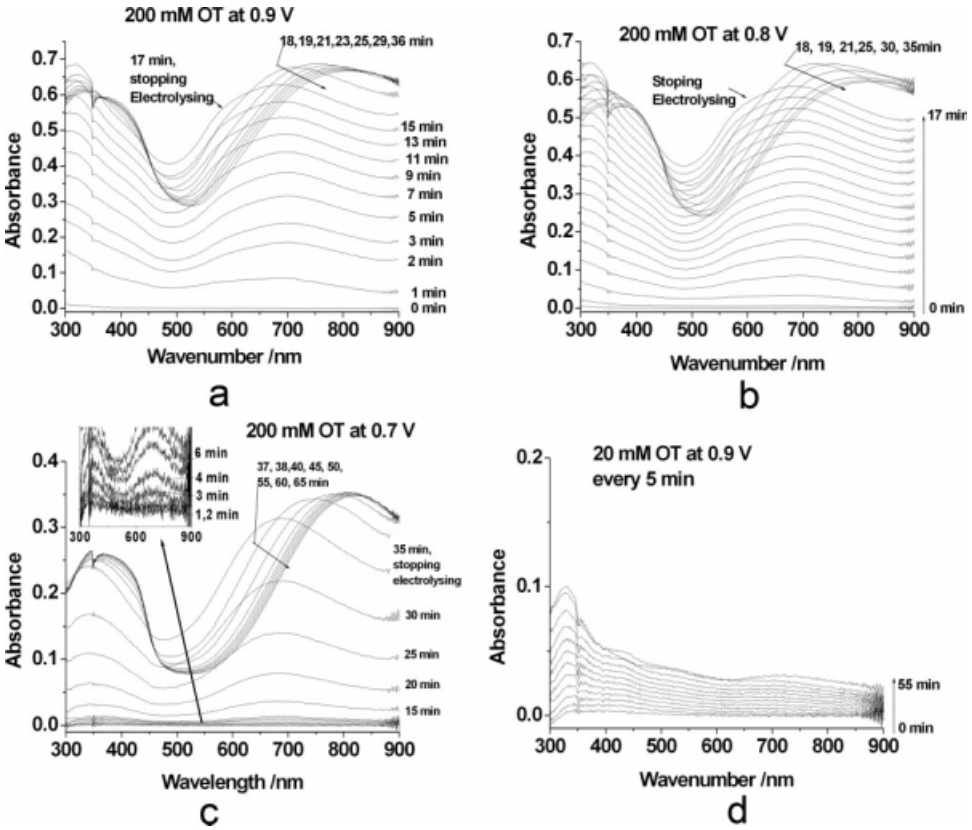

Figure 1 UV–vis absorption spectra recorded during constant potential electropolymerization of OT in a 0.5*M* sulfuric acid medium: (a) potential of 0.9 V and OT concentration of 200 m*M*, (b) potential of 0.8 V and OT concentration of 200 m*M*, (c) potential of 0.7 V and OT concentration of 200 m*M*, and potential of 0.9 V and OT concentration of 20 m*M*.

and were then characterized by FTIR spectroscopy and SEM. The FTIR spectra of the homopolymer and copolymer were collected directly through the placement of the ITO glass covered by the homopolymer/copolymer films on a Smart OMNI-Sampler (Madison, WI) attached to a Nicolet (Madison, WI) FTIR spectrometer (Nexus), which allowed fast, easy horizontal attenuated total reflectance analysis of all kinds of samples with a single-reflection crystal with a small sampling area. SEM was used to examine the surface morphology of the homopolymers/copolymers on the ITO glass with a Hitachi S-4800 microscope (Naka, Japan).

RESULTS AND DISCUSSION

In situ spectra of the homopolymerization of OT

Figure 1(a–c) shows the UV–vis spectra collected during the potentiostatic polymerization of 0.2 mol/L OT at potentials of 0.9, 0.8, and 0.7 V, respectively. After the start of electrolysis, two bands around 320 and 700 nm were obvious, which indicated that the poly(*o*-toluidine) (POT) was formed on the ITO electrodes. The bands around 320 and 700 nm were assigned to the π–π* transition[30,31] of the benzoic ring and to the polaronic transition[30,32–34] in POT, respectively. In comparison, the intensities of the absorption bands for 0.2*M* OT at potentials of 0.9 and 0.8 V increased faster than at a potential of 0.7 V. In addition, the plots of the absorbance at 700 nm in Figure 1(a–c) versus the electrolysis time shown in Figure 2 show that the absorbance of 700 nm at a

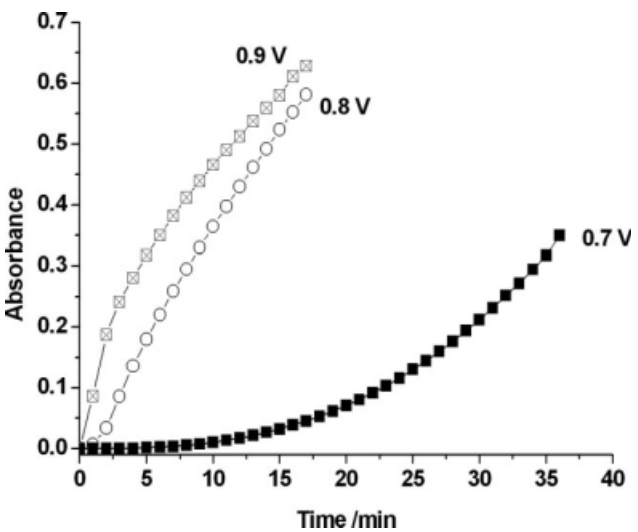

Figure 2 Time dependence of the absorbance at wavelength of 700 nm at different potentials in solutions containing OT at a concentration of 200 m*M*.

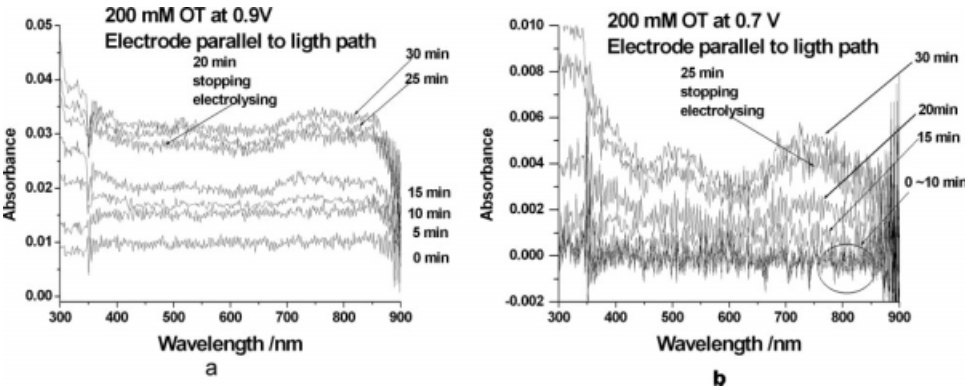

Figure 3 UV–vis absorption spectra recorded during the constant potential electropolymerization of OT with an ITO electrode parallel to the light path in a 0.5*M* sulfuric acid medium with an OT concentration of 200 m*M* and a potential of (a) 0.9 or (b) 0.8 V.

potential of 0.7 V began to increase evidently 10 min after constant electrolysis was started, which indicated that there was an induction period in the electropolymerization of OT similar to the chemical and electrochemical polymerization of aniline and its other derivatives.[35,36] The induction period was not obvious at higher potentials, that is, at 0.9 and 0.8 V, because of the faster electropolymerization of OT at higher potentials. During the electropolymerization of OT, the OT molecules first are oxidized to cation radical intermediates; then, they react with neutral OT molecules or each other to form dimers and oligomers in the orientations of head-to-head, tail-to-tail, and head-to-tail coupling. The head-to-tail coupling among the three coupling methods would cause chain propagation in the produced polymer on the ITO electrodes because the head-to-tail coupling predominates[37] when there are sufficient cation radicals near the electrode surface in solution or on the electrode surface. Hence, when the applied potential is higher, the OT cation radicals can be produced quickly because of the lower oxidation active energy at higher potential, which allows a large number of cation radicals to exist near the electrodes, and lead to the production of POT deposited on the ITO electrode. On the contrary, at lower potentials, the production of cation radicals is slower, so there are few cation radicals in the early stage of polymerization, which makes POT be produced quite slowly or not at all. However, after a longer electrolysis time, more cation radicals and some oxidation state oligomer gathering near or on the electrodes cause the polymerization reaction on the electrode to proceed more quickly, which is one of the reasons that the polymerization of aniline and its derivatives is autocatalysis reaction, as mentioned by some reports.[30,37–39] These conclusions also were supported by the *in situ* spectra shown in Figure 1(d), which were recorded during the electrochemical oxidation of OT in the solution with an OT concentration of 20 mmol/L at a potential of 0.9 V. The absorption band around 700 nm, shown in Figure 1(d), was not observed, but there was a weak absorption band around 320 nm, which indicated the π–π^* transition in the adjacently connected phenyl ring.[14] This showed that no sufficient amount of cation radicals was produced because of the lower OT concentration in solution so that POT did not grow, but the lower molecular weight oligomers of OT, such as dimers, trimers, and tetramers, should have been produced. This was in agreement with our study on the electropolymerization of aniline.[35] The spectra in the inset of Figure 1(c) show that, at the early stage of the electropolymerization of 200 mmol/L OT at a lower potential of 0.7 V, the absorption band around 320 nm appeared clearly earlier than that around 700 nm. This showed us that lower molecular weight oligomers grew before the formation of POT. They acted as intermediates and existed on the ITO glass electrode to form POT when their concentration was large enough.

Figure 3 shows *in situ* UV–vis spectra collected at applied constant potentials of 0.9 and 0.7 V, respectively, when the ITO glass work electrode was placed parallel to the light path. In contrast to the spectra shown in Figure 1(a–c), there were not obvious adsorption bands around 320 and 700 nm in Figure 3. We deduced that the POT was deposited on the ITO glass electrodes, as shown in Figure 1(a–c). The conclusion was supported by *in situ* UV–vis spectra recorded during the pulse electropolymerization of OT (not shown here). Upon the shift of potential to low potential in the pulse electropolymerization of OT, the adsorption bands in the UV–vis spectra recorded *in situ* shifted very quickly toward a longer wavelength, which meant that the POT film grew on the ITO glass electrode and experienced a transition from an oxidized state to a reduced state.

One shoulder band around 580 nm in the *in situ* UV–vis spectra was observed, as shown in Figure

1(a–c), during the electropolymerization of OT at a constant potential. The absorption bands at 580 nm were attributed to the transition from a localized benzenoid highest occupied molecular orbital to a quinoid lowest unoccupied molecular orbital,[40] that is, a benzenoid-to-quinoid excitonic transition,[41] in the polymer. This indicated that the produced POT on the electrode should have been in an oxidation state. As shown in Figure 1(a–c), the redshift of absorption band around 700 nm occurred in the succeeding *in situ* UV–vis spectra after the electrolysis of OT was stopped, and the shoulder bands around 580 nm also disappeared gradually, and the intensity of the absorption band between 400 and 420 nm grew. The absorption band between 400 and 420 nm was characteristic of the intermediate state,[42] through which the polymer of aniline or its derivatives turned from an oxidized to a reduced state, which involved the transition for polaron and bipolaron.[14,43–45] These phenomena suggest that the POT film produced by constant potential oxidation was in an oxidation state and possessed a cation radical structure, which proceeded the chemical reaction with the monomer of OT in the electrolyte solution to allow the POT film to have a lower oxidation degree.

In situ UV–vis spectra of the homopolymerization of PPDA

Several reports[46–50] have show that three phenylenediamine isomers all could be polymerized with chemical oxidation polymerization. The structure of the prepared polymers was the ladder structure[46–48] with phenazine type or the linear structure,[49,50] which closely relied on the oxidant and the media employed in the chemical oxidation polymerization. However, because the poly(*o*-phenylenediamine) or poly(*m*-phenylenediamine) deposited on the electrode through electropolymerization method was insulating, this led to a failure to produced electrochemically thicker and electroactive films on the electrode. The oligomer formed through the electropolymerization of PPDA is soluble in many solvents, so the formation of the film of poly(*para*-phenylenediamine) [poly(PPDA)] rarely happens by the electrochemical method.[48,51] As a result, a small number of studies on the electropolymerization of three phenylenediamine isomers was performed, but they could be electrochemically copolymerized with aniline and other aniline derivatives to form copolymers with unique physical and chemical properties,[52–54] such as conductivity, electrochromism, and the morphology of the polymer. In addition, PPDA can accelerate[40,55] the polymerization during its copolymerization with other aniline derivatives. Until now, there have been scarce reports about the electropolymerization of PPDA and its function in electrocopolymerization with *in situ* UV–vis spectra.

Figure 4(a) shows that there were absorption bands around 350 nm in the UV–vis spectra recorded during the electrooxidation of PPDA in solution containing 0.1 m*M* PPDA at a potential of 0.9 V, but the absorption bands were not observed in the UV–vis spectra shown in Figure 4(b) and collected during the electrooxidation of PPDA under conditions of the ITO glass electrode perpendicular to the light path. In addition, the *in situ* UV–vis spectra shown in Figure 4(c,d) were recorded during the electrooxidation of 2 m*M* PPDA at the lower potential of 0.7 V with the ITO electrode perpendicular or parallel to the light path, respectively. Only the UV–vis spectra shown in Figure 4(c) had the absorption band around 350 nm. This imply that the species represented by the absorption bands at 350 nm could only be produced and deposited on the ITO glass electrode in the previous two conditions. Usually, regardless of the electrooxidation and chemical oxidation of PPDA, the molecules of PPDA were first oxidized to form cation radicals; then, they coupled with each other (Scheme 1) through C—C, N—N and C—N bonding, which greatly depended on the reaction conditions.[46–50] Because of the low concentration of PPDA [0.1 m*M*; Fig. 4(a,b)] and low oxidation potential [0.7 V; Fig. 4(c,d)], not enough cation radicals were produced, and thus, no electropolymerization of PPDA occurred. However, as shown in Figure 4(a,c), the absorption bands around 350 nm generally could be attributed to the π–π^* transition in the adjacent connected phenyl ring, so this implies that the short chain molecules, such as dimers, trimers, and tetramer, might have formed and existed on the glass ITO electrode surface. They did not possess the structure of delocalized polarons with absorption bands in the long-wavelength region between 400 and 750 nm that characterize the formation of a long-chain polymer. Consequently, we hereby conclude that the species formed on the electrode came from routes 1 and 2 in Scheme 1 and that they could have been dimer molecules only adhering to the electrode in very small quantities.

Figure 4(e,f) presents the *in situ* UV–vis spectra recorded with an ITO glass electrode perpendicular and parallel to the light path, respectively, in 2 m*M* PPDA at a potential of 0.9 V. There were three absorption bands around 336, 470, and 665 nm, respectively, in Figure 4(e), whereas the absorption bands were around 336 and 528 nm in Figure 4(f). The absorption band around 528 nm is not clearly shown in Figure 4(e), like in Figure 4(f), because of its overlapping with the absorption band around 470 nm. These spectra were different than those shown in Figure 4(a–d) and were indicative of the fact that the species characterized by the absorption

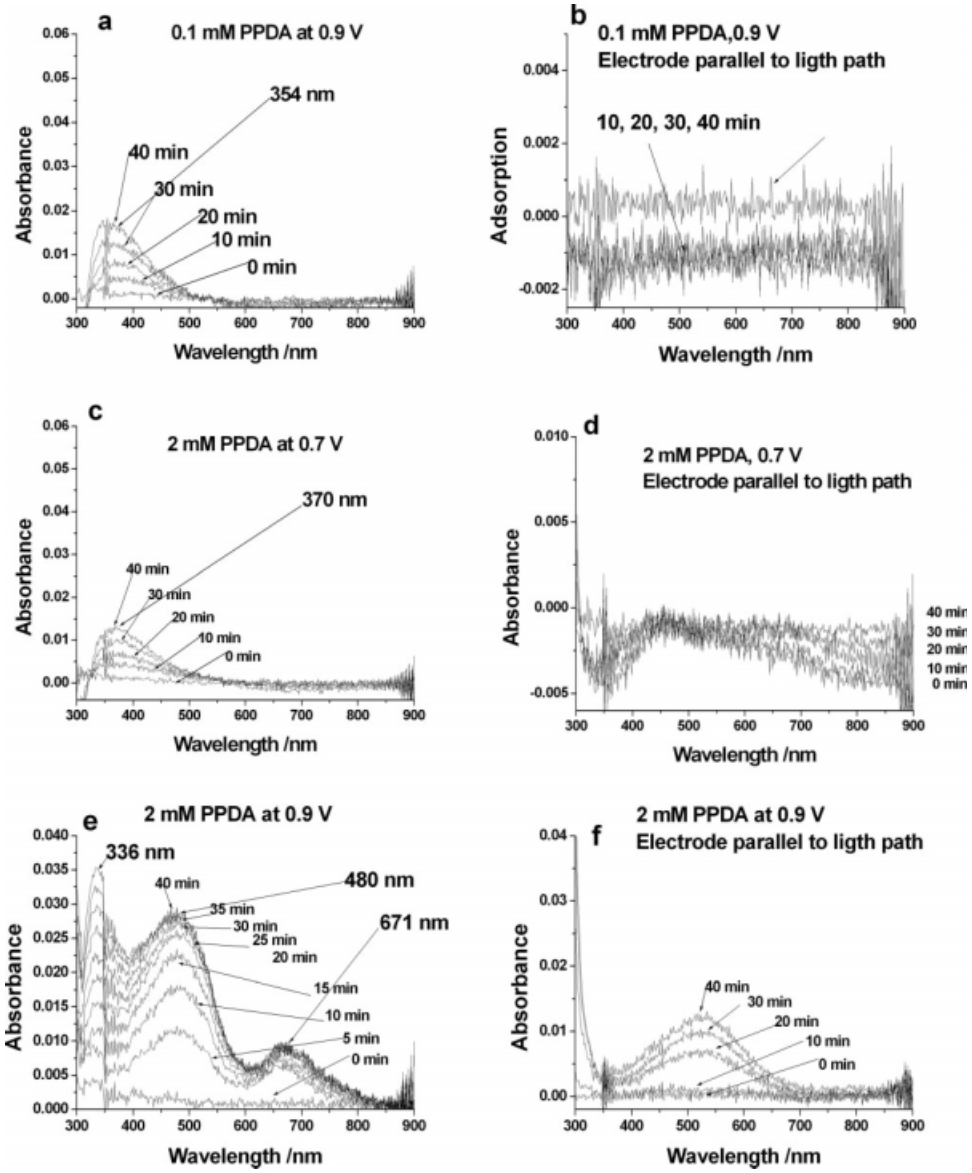

Figure 4 *In situ* spectra during the electrolysis of PPDA. The concentration of PPDA, potential, and electrode position with respect to the light path are labeled on the corresponding graphs.

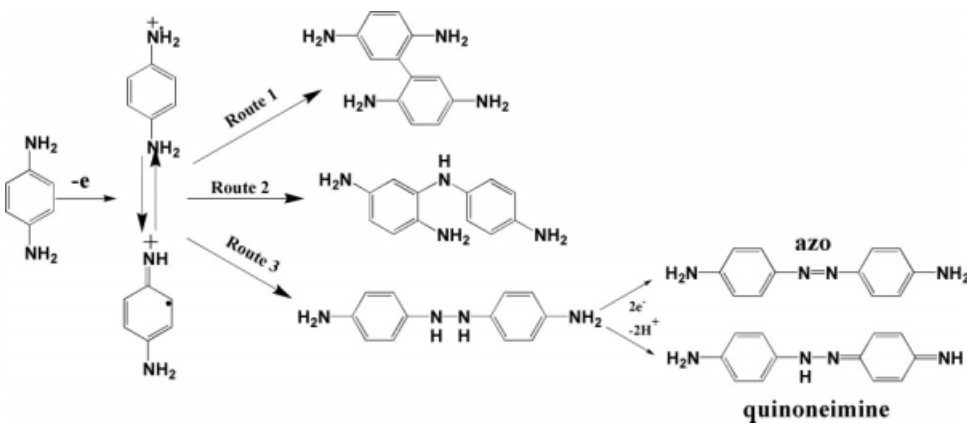

Scheme 1 Initial coupling routes during the electrolysis of PPDA.

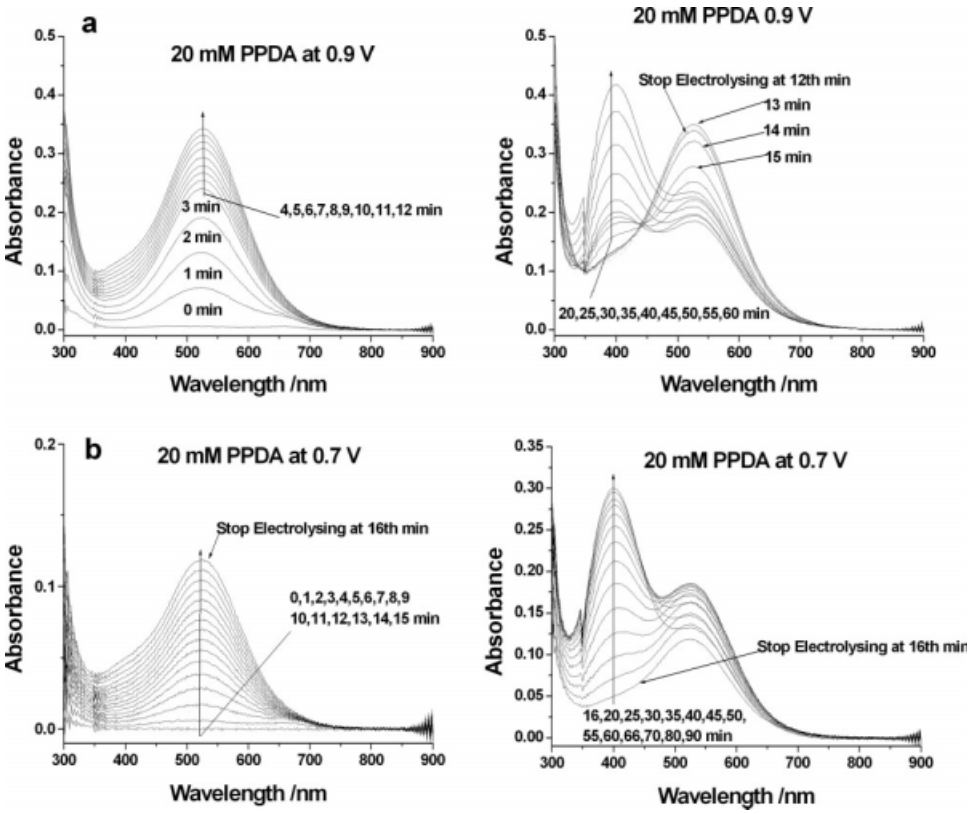

Figure 5 UV–vis spectra recorded in 20 m*M* PPDA at different potentials: (a) 0.9 and (b) 0.7 V.

bands in Figure 4(e) were solely on the electrode surface, whereas the species represented by the absorption bands around 528 nm were in solution. The former was some small oligomers with AZO structure, which were produced by the electrochemical oxidation of PPDA through route 3[49,50] in Scheme 1 and were present on the ITO glass electrode; the latter was oxidized poly(PPDA)[48] with a phenazine ladder structure generated by the electrochemical oxidation of PPDA through route 2 in Scheme 1 and was dissolved in electrolyte solution (discussed in detail later). As a result, this implies that poly(PPDA) was the main product when PPDA of a larger concentration was electrolyzed. This conclusion was supported by the *in situ* UV–vis spectra collected during the electrooxidation of PPDA at larger concentrations.

The *in situ* UV–vis spectra obtained during the electrolysis of 20 m*M* PPDA with the ITO glass electrode perpendicular to the light path at potentials of 0.9 and 0.7 V are shown in Figure 5(a,b), respectively. In the initial stage of electrolysis, there was the absorbance at 350 nm; the absorption shoulders around 500 and 660 nm were observed in the *in situ* UV–vis spectra. The two absorption bands were fast superposed by the absorption band around 528 nm and are clearer in Figure 5(a) than in Figure 5(b) because of the slower electrochemical oxidation at a 0.7-V potential than at a 0.9-V potential. This implies that the earlier performance of the electrolysis of 20 m*M* PPDA was similar to that described in Figure 4(e,f). Nevertheless, because the concentration of PPDA during the electrooxidation of PPDA was larger, 20 m*M*, a great number of cation radicals could have been generated rapidly to produce oxidized poly(PPDA), as represented by the absorption bands around 528 nm in Figure 5(a,b), through route 2 of Scheme 1. Cataldo[48] also observed that there were absorption bands around 528 nm in UV–vis spectra recorded during the polymerization of PPDA in sulfuric acid with the chemical oxidation method and thought that the absorption bands indicated the formation of oxidized poly(PPDA) with a phenazine ladder structure possessing a pernigraniline-like electronic structure. Therefore, we concluded reasonably that the poly(PPDA) characterized by the absorption bands around 528 nm in Figure 5(a,b) possessed same structure as suggested by Cataldo.[48] They were dissolved in solution because no deposited poly(PPDA) was observed on the ITO glass electrode after we stopped acquiring the *in situ* UV–vis spectra. From Figure 5(a,b), it is worth noting that after the electrolysis of PPDA was stopped, the absorption bands around 400 nm appeared, and its intensity increased, whereas the absorption intensity around 528 nm decreased. This showed that the

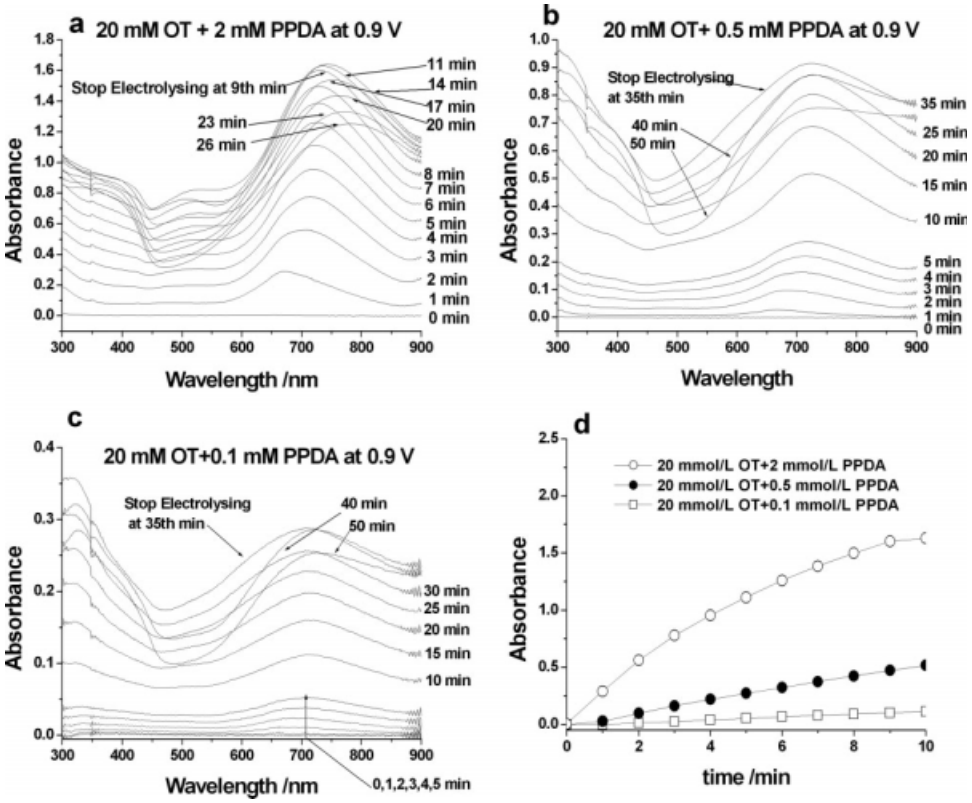

Figure 6 (a–c) *In situ* UV–vis spectra obtained during the electrocopolymerization of OT and PPDA at 0.9 V with a mixture of 20 m*M* OT and 2, 0.5, or 0.1 m*M* PPDA, respectively, and (d) time dependence of the absorbance at 700 nm in the UV–vis spectra.

oxidized poly(PPDA) continued to react with the PPDA monomer in solution after electrolysis was stopped to generate half-oxidized poly(PPDA) with an emeraldine electronic structure containing a polaron–π* transition, which resulted in the absorption bands around 400 nm in the UV–vis spectra [Fig. 5(a,b)] recorded uninterruptedly after the electrooxidation of PPDA was stopped. However, these phenomena did not occur in Cataldo's polymerization of PPDA with chemical oxidation[48] because of the presence of an oxidant in the whole process of the chemical oxidation of PPDA.

The material presented previously illustrates that the growth of species on the electrode and in solution during the electrooxidation of PPDA was clearly observed by the *in situ* UV–vis spectra. The UV–vis spectra shown in Figures 4 and 5 reveal that the practical processes and the species produced in the electrolysis of PPDA were influenced by the concentration of PPDA in solution and the potential applied.

In situ spectra of the electrocopolymerization of PPDA and OT

The UV–vis spectra collected during the potentiostatic electrocopolymerization of 20 m*M* OT with various concentrations of PPDA in the feed at 0.9 V of potential are shown in Figure 6. In comparison with the spectra shown in Figure 1(d), recorded during the electrolysis of 20 m*M* OT, the spectra in Figure 6 surprisingly indicate that the electrocopolymerization of PPDA and OT occurred because of the addition of PPDA to OT, which depended the concentration of PPDA. The absorption bands around 700 nm, pertinent to the polaron–π transition, observed in Figure 6(a–c) imply that there was mainly the POT type structure in the prepared polymer. However, there were obvious absorption bands around 528 nm, as shown in Figure 6(a), but these were not clear in Figure 6(b–c) and are not obvious in Figure 4(e). This indicates that the absorption bands around 528 nm shown in Figure 6 arose mainly from the copolymerization of PPDA and OT, which also imply the incorporation of PPDA units into the growing polymer and the formation of the phenazine type cyclic structure in the polymer according to the preceding discussion. Although the larger the concentration of PPDA in the feed was, the more phenazine-type cyclic structures there were in copolymer, the electrohomopolymerization did not occur for 2 m*M* PPDA and 20 m*M* OT, respectively, but there were some species produced on the electrode or in solution, according to the UV–vis spectra shown in Figures 1(d) and 4(e,f). The species

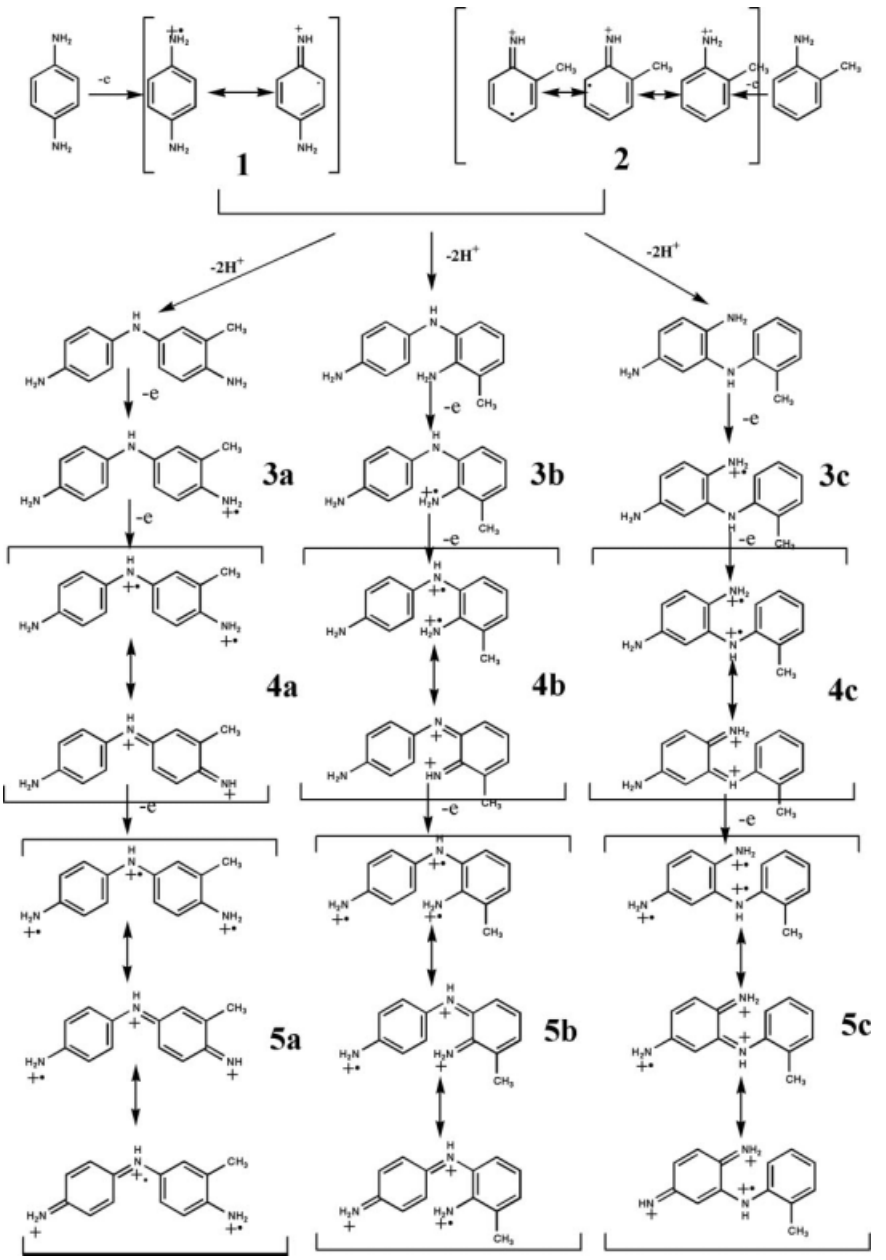

Scheme 2 Species involved in the copolymerization reaction between OT and PPDA.

should have been some kinds of intermediates, such as cation radicals and oxidized dimers or oligomers with cation radical structures. Therefore, we concluded that the intermediates, such as cation radicals resulting from the electrolysis of PPDA and OT, were able to couple each other to produce new kind of intermediates according to the coupling method shown in Scheme 2. The intermediates, such as **5a, 5b,** and **5c** shown in Scheme 2, may be considered kinds of more reactive electrophilic species that could more easily attack neutral OT, PPDA molecules, and OT or PPDA cation radicals to generate the copolymer more quickly. In the copolymer, there should have been structural units resembling **3a** that could produce UV–vis absorption bands around 700 nm, whereas there also should have been a phenazine-type cyclic structure in the copolymer resulting from the further oxidation of structural units, such as **3–5b** and **3–5c,** that could produce the UV–vis absorption bands around 520 nm.

The dependence of the absorption intensity around 700 nm in the UV–vis spectra for Figure 6(a–c) on the electrolysis time is shown Figure 6(d), which illustrates that the presence of PPDA not only caused copolymerization to occur, but also, the larger concentration of PPDA accelerated the copolymerization between PPDA and OT. From the UV–vis spectra in Figure 6(a–c), recorded continuously after

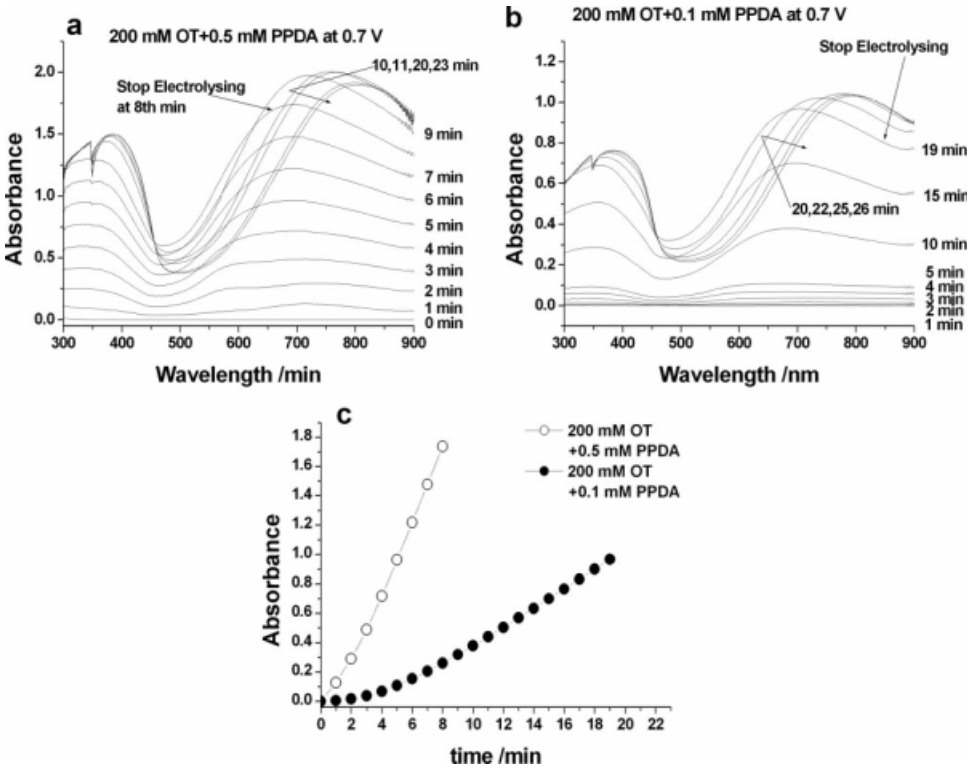

Figure 7 (a,b) *In situ* UV–vis spectra obtained during the electrocopolymerization of OT and PPDA at 0.7 V with a mixture of 200 m*M* OT and 0.5 or 0.1 m*M* PPDA, respectively, and (c) time dependence of the absorbance at 700 nm in the UV–vis spectra.

electrolysis was stopped, the redshift of the absorption band around 700 nm showed that the polymer produced on the ITO glass electrode was also in an oxidized state and continued to react with the neutral monomer molecule, which led to the appearance of the shoulder around 420 nm, which represented more polarons in polymer.

The *in situ* UV–vis spectra obtained during the potentiostatic electrocopolymerization of 200 m*M* OT with different concentrations of PPDA in the feed at a potential of 0.7 V are shown in Figure 7(a,b), and the plot of the absorption intensity at 700 nm in the UV–vis spectra versus electrolysis time is demonstrated in Figure 7(c). In comparison with the UV–vis spectra shown in Figure 1(d), the shape of the UV–vis spectra shown in Figure 7(a,b) was almost same, which indicated that there were mainly POT-type structural units and scarce phenazine-type cyclic units because of the very small PPDA concentration relative to the OT concentration in the feed, so no obvious absorption band around 528 nm was observed. However, the addition of PPDA to the OT solution sped up the electropolymerization of the mixture of PPDA and OT, as shown in Figure 7(c). Unlike the electrohomopolymerization of 200 m*M* OT, no obvious induction period for the mixture of 0.5 m*M* PPDA and 200 m*M* OT was observed. For a mixture of 0.1 m*M* PPDA and 200 m*M* OT, only about a 3-min induction period was observed, as shown in Figure 7(c)

From the previous discussion, we deduced that the cation radical intermediates generated during the anodic oxidation of PPDA or the mixture of PPDA and OT were very active, which caused and accelerated the copolymerization of PPDA and OT. We very reasonably concluded that the cation radical of PPDA produced electrochemically could react with neutral OT molecules or OT cation radicals generated by anodic oxidation, which formed intermediates more able to perform chain propagation to produce the polymers.

FTIR spectroscopy of the homopolymers and copolymers

The FTIR spectra of the homopolymer of POT and copolymer of OT and PPDA electrochemically deposited on the ITO glass electrode are presented in Figure 8. The characteristic bands in the FTIR spectra [Fig. 8(a–c)] for the POT and copolymer of OT and POT were assigned as follows:[56–58] the bands at about 1587 and 1492 cm^{-1} were indicative of stretching vibrations in the quinoid and benzoid rings, respectively; the bands at about 1324 and 1266 cm^{-1}

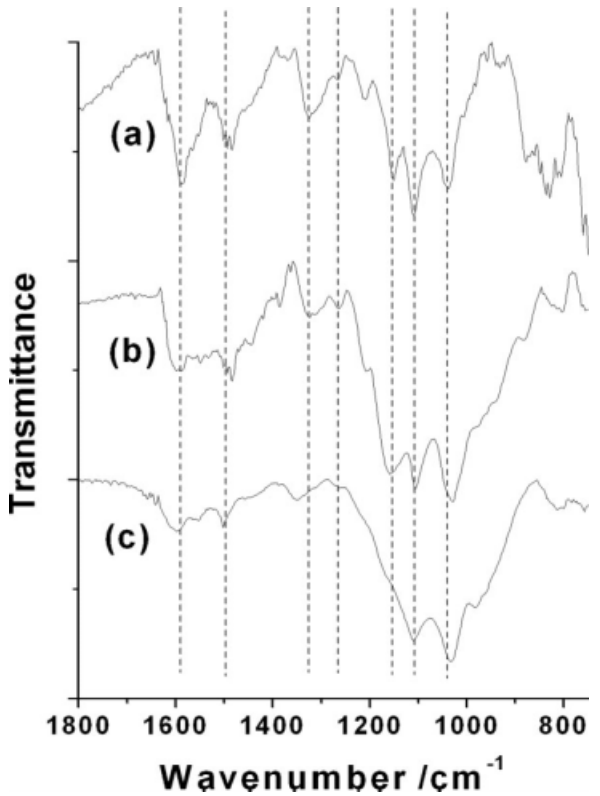

Figure 8 FTIR spectra of the polymer films deposited on ITO glass electrodes with the following electropolymerization conditions: (a) 200 m*M* OT and 0.9 V; (b) 200 m*M* OT, 0.5 m*M* PPDA, and 0.7 V; and (c) 20 m*M* OT, 2 m*M* PPDA, and 0.9 V.

were attributed to C—N stretching vibrations in the quinoid and benzoid rings, respectively; the bands at about 1151 and 1109 cm^{-1} represented C—H out-of-plane and in-plane bend vibration benzoid rings; the bands at 808 cm^{-1} illustrated the occurrence of parasubstitution, which proved the formation of the polymer; and the bands around 1037 cm^{-1} revealed the presence of 1,2,4-trisubstitution[57] in the POT and copolymer of OT and PPDA because of the presence of OT units in the polymers.

In general, we considered the bands between 600 and 1000 cm^{-1} to be relative to C—H bend vibration in benzoid rings, and their variation illustrated that more multiple substitution, such as tetra substitution in the benzoid ring, occurred for the copolymer.[49] By comparison with the FTIR spectra of POT [Fig. 8(a)], the bands at about 1151, 1109, and between 750 and 1000 cm^{-1} in the FTIR spectra of the copolymer [Fig. 8(b,c)] changed obviously; which illustrated that there were tetra-substituted benzoid rings in the polymer arising from the electrocopolymerization of PPDA and OT. In particular, the bands at about 1151 and 1109 cm^{-1} became less obvious with increasing ratio of [PPDA] to [OT] in the feed. This showed that the number of tetra-substituted benzoid rings increased with the ratio of [PPDA] to [OT] in the feed. The tetra-substituted benzoid ring could have had a phenaziline-like cyclic structure, which was formed by the combination of the PPDA unit with the OT or PPDA unit (Scheme 3). This conclusion was consistent with the results represented by the UV–vis spectra in Figure 6(a–c) and the discussion for them.

SEM images of the homopolymers and copolymers

The SEM images of the electrochemically prepared POT on the ITO glass electrode in 200 m*M* OT solution at potentials of 0.9 and 0.7 V are shown in Figure 9(a,b), respectively, which reveal that the morphology of the polymer could have been related to the employed potential during electropolymerization. A slight difference in the two SEM images was observed. As shown in Figure 2, the higher potential resulted in the faster electrohomopolymerization of OT, which led to the faster nucleation of polymers, so the prepared polymer at 0.9 V had a less porous surface than that at 0.7 V.

The SEM images of the electrochemically prepared copolymer in 20 m*M* OT + 2 m*M* PPDA at 0.9 V and in 200 m*M* OT + 0.5 m*M* solution at 0.7 V are shown in Figure 9(c,d), respectively. In comparison with Figure 9(a,b), the images in Figure 9(c,d) reveal that PPDA not only could be electrocopolymerized with OT but also produced the copolymer with a fibroid surface morphology. Furthermore, the fibroid surface morphology was more visible with higher ratios of [PPDA] to [OT] in the feed. Figure 9(c) shows that the diameter and the length of

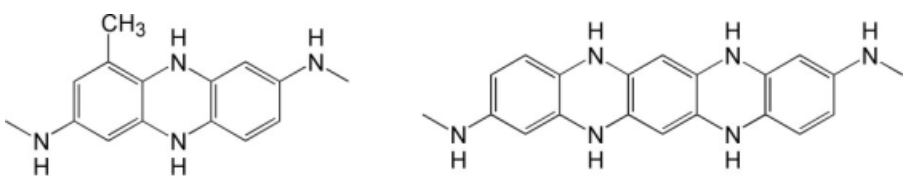

Scheme 3 Structural units in the copolymer of OT and PPDA.

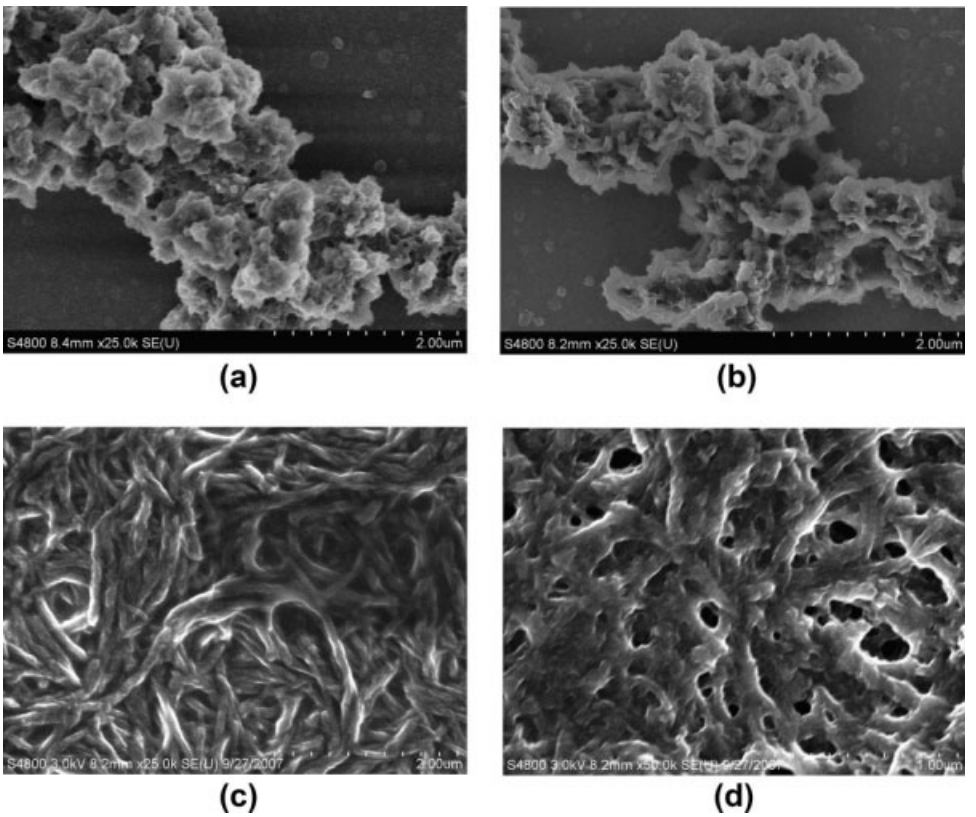

Figure 9 SEM images of the polymer films deposited on ITO glass electrodes with the following electropolymerization conditions: (a) 200 m*M* OT and 0.9 V; (b) 200 m*M* OT and 0.7 V; (c) 20 m*M* OT, 2 m*M* PPDA, and 0.9 V; and (d) 200 m*M* OT, 0.5 m*M* PPDA, and 0.7 V.

fibroid-shaped particles for the copolymer reached about 100 and 1000 nm, respectively. From the SEM images, FTIR spectra of the polymers, and *in situ* UV–vis spectra during electropolymerization, we deduced that the electrocopolymerization between PPDA and OT definitely happened, and that its mechanism was different from that of the electrohomopolymerization of PPDA and OT. The growth of a phenaziline-like cyclic structure in the copolymer was in favor of the formation of a long chain to produce a fibroid surface morphology for the copolymers. This kind of long chain was suggested to be able to improve the conductivity of copolymers.[59]

CONCLUSIONS

This study showed that the potentiostatic electrohomopolymerization of PPDA and OT on an ITO glass electrode can be performed, which was closely related to the applied potential and monomer concentration. An induction period was visible for the polymerization of OT with the potentiostatic electrolysis method when the applied potential was lower. When the concentration of OT was very small, the electropolymerization of OT could not be carried out, but the *in situ* UV–vis spectra collected showed that some species, such as dimers and other short-chain oligomers, with adjacent phenyl ring structures were produced on the ITO glass electrode, which were suggested to be the intermediates in the electropolymerization of OT. The *in situ* UV–vis spectra recorded during the electrolysis of PPDA indicated that the electropolymerization of PPDA occurred, and the prepared poly(PPDA) had phenaziline cyclic structure units by C—N coupling. The FTIR spectra of the polymers and the *in situ* UV–vis spectra obtained during the electrochemical copolymerization of PPDA and OT showed that the copolymer of OT and PPDA was prepared electrochemically and had phenaziline-like cyclic structure units resulting from the cyclization of the adjacent PPDA and OT or the presence of poly (PPDA) blocks in the copolymer chain. The occurrence of the electrochemical copolymerization of PPDA and OT was supported by the SEM images of the polymer produced with anodic electrolysis of the mixture of PPDA and OT because the images showed that the copolymer possessed a fibroid surface morphology.

References

1. Riul, A., Jr.; Soto, A. M. G.; Mello, S. V.; Bone, S.; Taylor, D. M.; Mattoso, L. H. C. Synth Met 2003, 132, 109.
2. Yasuda, A.; Shimidzu, T. Polym J 1993, 25, 329.
3. Cao, Y.; Andreatta, A.; Heeger, A. J.; Smith, P. Polymer 1989, 30, 2305.
4. Ma, X. Y.; Shi, W. L. Microelectron Eng 2003, 66, 153.
5. Anderson, M. R.; Mattes, B. R.; Reiss, H.; Kaner, R. B. Science 1991, 252, 1412.
6. Sharma, S. K.; Misra, S. C. K.; Tripathi, K. N. J Nonlinear Opt Phys 2003, 12, 39.
7. Saxena, V.; Malhotra, B. D. Curr Appl Phys 2003, 3, 293.
8. Thanneermalai, M.; Jeyaraman, T.; Sivakumar, C.; Gopalan, V. A.; Wen, T. T. C. Spectrochim Acta A 2003, 59, 1937.
9. Wei, Y.; Hariharan, R.; Patel, S. A. Macromolecules 1990, 23, 758.
10. Pekmez-Özcicek, N.; Pekmez, K.; Holze, R.; Yildiz, A. J Appl Polym Sci 2003, 89, 862.
11. Sahin, Y.; Percin, S.; Sahin, M.; Ozkan, G. J Appl Polym Sci 2004, 91, 2302.
12. Malinauskas, A.; Bron, M.; Holze, R. Synth Met 1998, 92, 127.
13. Savita, P.; Sathyanarayana, D. N. Polym Int 2004, 53, 106.
14. Savita, P.; Sathyanarayana, D. N. Synth Met 2004, 145, 113.
15. Tang, H.; Kitani, A.; Maitani, S.; Munemura, H.; Shiotani, M. Electrochim Acta 1995, 40, 849.
16. Mazeikiene, R.; Malinauskas, A. Synth Met 1998, 92, 259.
17. Probst, M.; Holze, R. Macromol Chem Phys 1997, 198, 1499.
18. Ogura, K.; Kokura, M.; Nakayama, M. J Electrochem Soc 1995, 142, L152.
19. Borole, D.; Kapadi, U. R.; Mahulikar, P. P.; Hundiwale, D. G. Polym Adv Technol 2004, 15, 306.
20. Elia, L. F. D.; Ortiz, R. L.; Marquez, O. P.; Marquez, J.; Martinez, Y. J Electrochem Soc 2001, 148, C297.
21. Sivakkumar, S. R.; Saraswathi, R. J Appl Electrochem 2004, 34, 1147.
22. Genies, E. M.; Lapkowski, M. J Electroanal Chem 1987, 236, 189.
23. Malinauskas, A.; Holze, R. Electrochim Acta 1999, 44, 2613.
24. Malinauskas, A.; Holze, R. Besenges B Phys Chem 1997, 101, 1859.
25. Malinauskas, A.; Holze, R. Electrochim Acta 1998, 43, 2413.
26. Wu, M. S.; Wen, T. C.; Gopalan, A. Mater Chem Phys 2002, 74, 58.
27. Wen, T. C.; Sivakumar, C.; Gopalan, A. Electrochim Acta 2001, 46, 1071.
28. Shah, A. A.; Holze, R. Synth Met 2006, 156, 566.
29. Santhosh, P.; Sankarasubramanian, M.; Thanneermalai, M.; Gopalan, A.; Vasudevan, T. Mater Chem Phys 2004, 85, 316.
30. Bilal, S.; Holze, R. Electrochim Acta 2007, 52, 5346.
31. Kumar, D. Eur Polym J 2001, 37, 1721.
32. Rao, P. S.; Subrahmanya, S.; Sathyanarayana, D. N. Synth Met 2002, 128, 311.
33. Karatchevtseva, I.; Zhang, Z.; Luca, J. X.; Luca, V. Chem Mater 2006, 18, 4908.
34. Kinyanjui, J. M.; Wijeratne, N. R.; Hanks, J.; Hatchett, D. W. Electrochim Acta 2006, 51, 2825.
35. Zhang, G. R.; Wang, H.; Liu, X. L.; Lu, J.-X. Acta Polym Sinica 2008, 1, 41.
36. Shreepathi, S.; Holze, R. Langmuir 2006, 22, 5196.
37. Yang, H.; Bard, A. J. J Electroanal Chem 1992, 339, 423.
38. Yoo, J. S.; Song, I.; Lee, J. H.; Park, S. M. Anal Chem 2003, 75, 3294.
39. Kennedy, A.; Glidle, B.; Cunnane, V. J. J Electroanal Chem 2007, 608, 22.
40. Stejskal, J.; Kratochvìl, P.; Špírkovát, M. Polymer 1995, 36, 4135.
41. Stejskal, J.; Trchová, M.; Prokeš, J.; Sapurina, I. Chem Mater 2001, 13, 4083.
42. Lu, X.; Yu, Y.; Chen, L.; Mao, H.; Zhang, W.; Wei, Y. Chem Commun 2004, 1522.
43. Mallick, K.; Witcomb, M. J.; Scurrell, M. S. Eur Polym J 2006, 42, 670.
44. Hasik, M.; Wenda, E.; Bernasik, A.; Kowalski, K.; Sobczak, J. W.; Sobczak, E. Polymer 2003, 44, 7809.
45. Dufour, B.; Rannou, P.; Travers, J. P.; Pron, A. Macromolecules 2002, 35, 6112.
46. Prokeš, J.; Stejskal, J.; Křivka, I.; Tobolková, E. Synth Met 1999, 102, 1205.
47. Sulimenko, T.; Stejskal, J.; Prokeš, J. J Colloid Interface Sci 2001, 236, 328.
48. Cataldo, F. Eur Polym J 1996, 32, 43.
49. Ichinohe, D.; Muranaka, T.; Sasaki, T.; Kobayashi, M.; Kise, H. J Polym Sci Part A: Polym Chem 1998, 36, 2593.
50. Ichinohe, D.; Saitoh, N.; Kise, H. Macromol Chem Phys 1998, 199, 1241.
51. Li, X.-G.; Huang, M.-R.; Duan, W.; Yang, Y.-L. Chem Rev 2002, 102, 2925.
52. Tang, H.; Kitani, A.; Maitani, S.; Munemura, H.; Shiotani, M. Electrochim Acta 1995, 40, 849.
53. Zhang, G.-R.; Xu, C.-T.; Zhang, A.-J.; Chen, L.; Lu, J. X. Acta Chim Sinica 2008, 66, 376.
54. Yang, C.-H.; Wen, T.-C. J Appl Electrochem 1994, 24, 166.
55. Tang, H.-Q.; Kitani, A.; Aitani, S.; Munemura, H.; Shiotani, M. Electrochim Acta 1995, 40, 849.
56. Kulkarni, M. V.; Viswanath, A. K. Eur Polym J 2004, 40, 379.
57. Borole, D. D.; Kapadi, U. R.; Mahulikar, P. P.; Hundiwale, D. G. Spectrochim Acta A 2007, 66, 37.
58. Borole, D. D.; Kapadi, U. R.; Mahulikar, P. P.; Hundiwale, D. G. Mater Lett 2006, 60, 2447.
59. Tang, H.; Kitani, A.; Miaitani, S.; Munemura, H.; Tshiotani, M. Electrochim Acta 1995, 40, 849.